Development 125, 4303-4312 (1998)
Printed in Great Britain © The Company of Biologists Limited 1998
DEV0184

Non-autonomy of *AGAMOUS* function in flower development: use of a Cre/*loxP* method for mosaic analysis in *Arabidopsis*

Leslie E. Sieburth[1,2,§], Gary N. Drews[2,*] and Elliot M. Meyerowitz[2]

[1]Department of Biology, McGill University, 1205 Dr Penfield Avenue, Montreal, PQ Canada H3A 1B1
[2]Division of Biology 156-29, California Institute of Technology, Pasadena, CA 91125, USA
*Present address: Department of Biology, University of Utah, Salt Lake City, UT 84112, USA
[§]Author for correspondence

Accepted 10 August; published on WWW 30 September 1998

SUMMARY

Angiosperms use a multi-layered meristem (typically L1, L2 and L3) to produce primordia that then develop into plant organs. A number of experiments show that communication between the cell layers is important for normal development. We examined whether the function of the flower developmental control gene *AGAMOUS* involves communication across these layers. We developed a mosaic strategy using the Cre/*loxP* site-specific recombinase system, and identified the sector structure for mosaics that produced mutant flowers. The major conclusions were that (1) *AGAMOUS* must be active in the L2 for staminoid and carpelloid tissues, (2) that *AGAMOUS* must be active in the L2 and the L3 for floral meristem determinacy, and (3) that epidermal cell identity can be communicated by the L2 to the L1 layer.

Key words: Flower development, *AGAMOUS*, Genetic mosaics, *Arabidopsis*, Meristem

INTRODUCTION

In most plant species, flowers are composed of four different organ types. These organs are sepals, petals, stamens and carpels, and they are arranged in concentric rings termed whorls. In *Arabidopsis*, the first (outer) whorl contains four sepals, the second whorl four petals, the third whorl six stamens, and the fourth (inner) whorl two fused carpels. We have been using *Arabidopsis thaliana* as a system to study the genetic control of floral organ pattern.

Genes specifying floral organ identity have been identified through the isolation and characterization of floral homeotic mutants (reviewed by Coen and Meyerowitz, 1991). These mutants show floral-organ-specification defects in two adjacent whorls; mutations in the *APETALA1* and the *APETALA2* genes cause defects in whorls 1 and 2, mutations in the *APETALA3* and *PISTILLATA* genes cause defects in whorls 2 and 3, and mutations in the *AGAMOUS* (*AG*) gene cause defects in whorls 3 and 4. In plants mutant for *AG*, third whorl organs develop as petals rather than stamens and another (mutant) flower is produced in the place of fourth whorl carpels. The fourth whorl defects thus include both changes in organ identity (loss of specification of carpels) and the loss of floral meristem determinacy (failure to cease proliferation after the production of four whorls of organs).

Floral primordia arise from the undifferentiated cells of the apical meristem. For many angiosperms, this structure is organized into three clonally distinct sets of cells that are organized into layers (called the L1, the L2 and the L3; Satina et al., 1940). In the meristem, the L1 and L2 are each single cell layers that are maintained by anticlinal cell divisions. In contrast, the L3 comprises the central core of the meristem, and these cells are not constrained with respect to their cell division orientations. Floral organ primordium initiation is accompanied by changes in cell division patterns; each organ receives a characteristic contribution of cells from each layer, with the L1 contributing the epidermal cells, the L2 cells the subepidermal layer, and the L3 the core of some tissues (Satina et al., 1940; Satina, 1944; Derman and Stewart, 1973).

In situ hybridization studies have revealed that *AG* RNA first accumulates uniformly in the central region of young (stage 3) flower primordia (Drews et al., 1991; flower stages according to Smyth et al., 1990). This expression domain includes L1, L2 and L3 meristematic layers, and corresponds to the region of the floral meristem that will give rise to stamens and carpels. The fact that each floral organ receives a predictable contribution from each of the three meristematic layers suggests the existence of a mechanism for coordinating proliferation among the cell layers. The timing of *AG* expression, and the homeotic defects observed upon loss of *AG* function suggests that *AG* may contribute to this process. One approach to address whether *AG* does play a role in communication of developmental information among the meristematic (L1-L3) layers is to determine where it must be expressed for normal development. We are addressing this question through the analysis of *AG* mosaics.

To determine where *AG* must be expressed for normal development, we used the Cre site-specific recombinase of

bacteriophage P1 to develop a genetic mosaic system. We tested this system, and used it to generate plants in which the only functional copy of *AG* was restricted to one or two of the three meristematic layers. The analysis of the mosaic flowers showed that for formation of staminoid and carpelloid tissues, *AG* expression in the L2 was essential, and to achieve floral meristem determinacy, *AG* had to be expressed in both the L2 and the L3. These observations lead to the development of models for *AG* function in which different activities result in determinacy and stamen and carpel development.

MATERIALS AND METHODS

Lox target site vector construction

Target site constructs were designed to have direct repeats of the *loxP* sites to exploit the deletion activity of the Cre recombinase (Sternberg and Hamilton 1981). An oligonucleotide containing these repeats (underlined) with accompanying restriction sites (5′) AAGCTTATAACTTCGTATAGCATACATTATACGAAGTTATCTGCAGTCTAGAGGATCCGTTTAAACATAACTTCGTATAGCATACATTATACGAAGTTATGGTACC was synthesized and cloned into pGEM7zf(+), creating pGEMLox1. A 35S::GUS fragment derived from pBI221 (CLONTECH) was inserted into the *Pst*I site of pGEMLox1, and clones containing GUS in each orientation were recovered (pGEMLox2a and pGEMlox2b). The *loxP*/GUS regions were subcloned into the pCGN1578 plant transformation vector (McBride and Summerfelt 1990) to produce pCGNLox2a and pCGNlox2b. These clones contain a unique *Pme*I site adjacent to 35S::GUS for the insertion of any gene of interest. We used this restriction site to insert an engineered version of *AG* (described previously; Sieburth et al., 1995) into the pCGNLox2b construct. A diagram of the final AGLox construct is shown in Fig. 1B.

Heat shock-CRE recombinase gene fusion

To provide inducible expression of the Cre site-specific recombinase, we fused the CRE coding region to the heat shock promoter HSP18.2 (Takahashi and Komeda 1989). This was done by a two-step PCR mutagenesis. The first step used oligos with sequences of both CRE and HSP18.2. The heat shock promoter fragment was amplified from pTT119 (Takahashi and Komeda 1989) using oligonucleotides 116 [(5′) GGTCAGTAAATTGGACATTGTTCGTTGCTTTTC] and T3. Amplification of the primary CRE fragment was performed using oligonucleotides 117 [(5′) GAAAAGCAACGAACAATGTCCAATTTACTGACC, underlined portions of oligonucleotides 116 and 117 correspond to CRE, and the non-underlined portions correspond to HSP18.2] and 033: [(5′) TTCGAACGCTAGAGCCTG]. The fusion product was generated and amplified using the two primary products, and the 033 and T3 oligonucleotides. The fusion product and the remainder of the CRE coding region were reassembled and placed upstream of a 3′ NOS terminator using standard protocols. The final product was inserted into the pCGN 1547 plant transformation vector (McBride and Summerfelt 1990) to produce pCGNHCN.

Plant transformation

Lines of transgenic plants carrying each construct were established using Agrobacterium-mediated transformation. Root tissue of the *Arabidopsis* ecotype Nossen was cultured in liquid medium, and used for transformation following established protocols (Valvekens et al., 1988). The insert copy number was assessed by analysis of kanamycin resistance segregation and, in some cases, by DNA gel blots (data not shown).

Molecular detection of recombination

Oligonucleotide pairs were designed to assay for the presence of the HS::CRE recombinase construct, the original *loxP* target site construct, and the recombined target site product. These pairs are: 117: GAAAAGCAACGAACAATGGGATATTCAACTGCT and 033: TTCGAACGCTAGAGCCTG (for a 400 bp Cre-specific product); GUS802: CCGGGATCCATCGCAGCGTA and GD25: GGTTTTTGTCACGCGCTA (for a 702 bp non-recombined target site-specific product); and TML648 GCCAGACTTAGTGTGTAGAT and the M13 reverse primer (for a 330 bp recombination-specific product). DNA was isolated from inflorescence tissue (Dellaporta et al., 1983) of both control (non-heat-shocked) and heat-shocked plants carrying the two transgenes.

Heat-shock induction of Cre site-specific recombinase

To induce expression of the Cre site-specific recombinase, plants were immersed in warm water. To test for recombination during embryogenesis, inflorescences carrying siliques were immersed in water at 39.5°C for 3 hours. To test for transmission of a recombined sector into inflorescence tissue, 10-day seedlings were placed into weighted plastic bags and immersed into a 39.5°C water bath for 4 hours. Immediately following the heat shock, these plants were repotted, and maintained at 20°C until flowering. To induce Cre expression for generation of *ag* mosaic plants, F_1 seeds were germinated on plates of sterile MS-Kan (0.5× MS salts [Sigma], 0.8% Phytagar [Gibco/BRL], 50 mg/l kanamycin) and plates carrying 4-day-old seedlings were sealed with parafilm and immersed in 39-40°C water for 2-4 hours [no difference in frequency of mutant flowers or complexity of sector configuration was observed for these HS treatments (data not shown)]. All seedlings were transferred to soil when 7-days old, and grown to flowering. Flowers on the primary and the first two secondary inflorescences were scored for defects in the identity of third and fourth whorl organs. Inflorescences were then stained for GUS activity and examined as described previously (Sieburth and Meyerowitz, 1997).

Microscopy and image preparation

Sectioned plant material was viewed under either darkfield illumination or using DIC optics with an Olympus BX50 microscope. Slides of plant material were digitized using a Nikon Coolscan II, and assembled into composites using Photoshop 4.0.

RESULTS

Cre/*loxP* genetic mosaic system

Our goal was to determine whether the developmental function of *AGAMOUS* (*AG*) involves communication among the L1, L2 and L3 cell layers of the floral meristem. To address this question, we generated mosaic plants containing cell layer sectors mutant for the *AG* gene. Our strategy is outlined in Fig. 1A, and was based on a method first used with the FLP recombinase in *Drosophila* (Golic and Lindquist, 1989). Instead of using FLP, we used the Cre site-specific recombinase from bacteriophage P1, which has been shown previously to function in plants (Odell et al., 1990; Russell et al., 1992).

We placed an engineered copy of the *AG* gene (under the control of its own promoter; Sieburth et al., 1995) and a cell-autonomous reporter gene (35S::GUS; Jefferson et al., 1987) between two *loxP* sites (AGLox; Fig. 2B) and introduced this construct into *ag* mutant plants. We then supplied these plants with the Cre site-specific recombinase, which acts upon the *loxP* direct repeats, resulting in excision of the intervening sequences (the *AG* and 35S::GUS genes) (Sternberg and Hamilton, 1981). Because excision results in the cell failing to

produce the GUS staining product, GUS staining allowed distinction between *AG*-containing and *AG*-deficient sectors. To control the level and timing of Cre site-specific recombinase expression, we placed the CRE coding region under the control of a heat shock promoter (HS::CRE, Fig. 1C) and heat-shocked plants to induce Cre expression.

Heat shock induces GUS(–) sectors during embryogenesis

We performed a histological test to determine whether the system functioned as expected. F_1 embryos that combined single copies of both the AGLox and the HS::CRE constructs were generated by crosses between the appropriate plants, and were heat shocked within the first week following pollination. The resultant seeds were germinated and 7-day-old seedlings were stained for GUS activity. Both non-heat-shocked F_1 seedlings, and heat-shocked selfed AGLox plants were uniformly blue, as is expected from plants carrying a 35S::GUS transgene (Fig. 2A). By contrast, the seedlings from heat-shocked F_1 embryos showed prominent white sectors (Fig. 2B-D). These large white sectors are consistent with the early stage of embryo development at which the heat shock was administered. These results indicated that heat shock induced expression of the HS::CRE transgene, and that excision resulted in loss of GUS staining.

Recombined sectors are transmitted to the inflorescence

Because our goal was to analyze sectors affecting flower development, it was important to obtain large inflorescence sectors. In the embryo, a small subset of the shoot apical meristem cells gives rise to large portions of the inflorescence (Irish and Sussex 1992; Furner and Pumfrey 1993); therefore we reasoned that inducing recombination early in development would maximize the likelihood that large inflorescence clonal sectors could be recovered. To test whether heat-shock provided early during seedling development would give rise to sectors within the inflorescence, DNA isolated from inflorescence tissue 4 weeks after a heat shock was used in PCR reactions. These reactions were designed to detect the HS::CRE construct, and the *loxP*-containing construct in both its original and the predicted recombined configuration (Fig. 3A). The results from reactions using two control plants (no heat shock) and one heat-shocked plant are shown in Fig. 3B. The CRE recombinase transgene (lanes C) and the non-recombined *loxP* construct (lanes N) were detected in all plant tissues tested, however the R (recombined) product was never detected in DNA from control plants, and was detected in approximately half of the heat-shocked plants. These results indicated that the anticipated recombination event had occurred, that meristematic cells contributing to the inflorescence could be induced to undergo recombination, and that recombination occurred in only a subset of meristematic cells, leading to mosaic plants containing both recombined and non-recombined sectors.

Sector identification

To be assured that changes in GUS expression reflected Cre-mediated excision, we analyzed the activity of the 35S promoter in floral tissue. Although considered to be a constitutive promoter, both developmental and tissue-specific patterns of 35S-driven expression have been noted in early seedling development (Benfey et al., 1989, 1990). Fig. 4A shows the typical low levels of GUS staining in the inflorescence meristem. As flowers developed, we observed a steady increase in accumulation of the GUS staining product (Fig. 4B-E). In mature flowers, sepals showed nearly uniform GUS staining (Fig. 4C), petals gave a low level of staining (data not shown; also reported by Bossinger and Smyth, 1996), stamens showed generally high levels of staining (Fig. 4D), and carpel GUS staining was somewhat variable (Fig. 4E). The abundant GUS staining in sepals and the receptacle late in flower development allowed us to use these tissues to deduce sector configurations.

We based our assignment of sector structure on previously

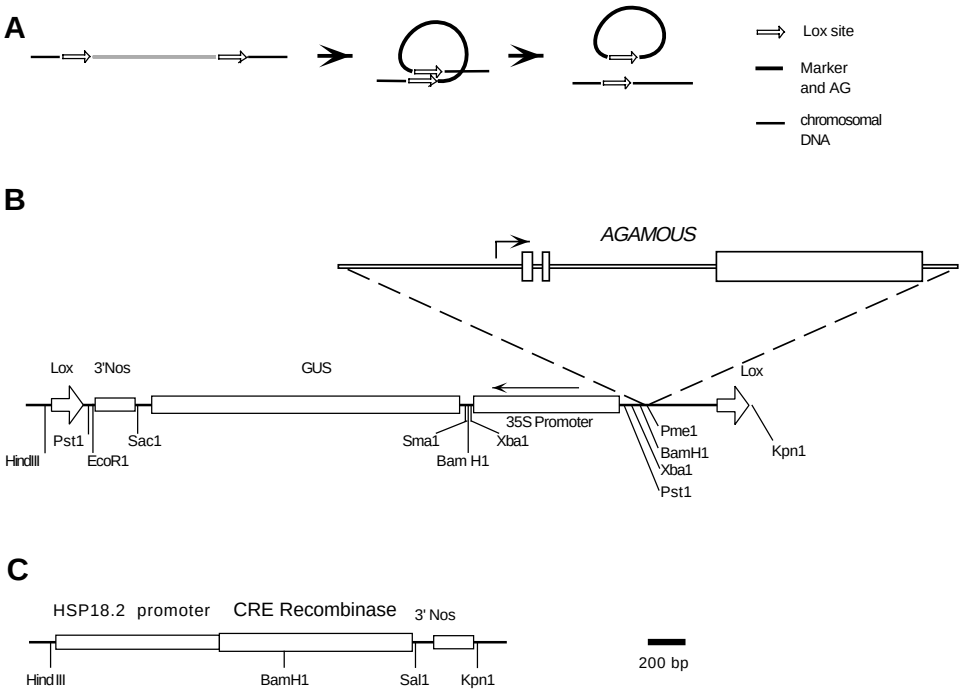

Fig. 1. Strategy and constructs for Cre/*loxP* genetic mosaic analysis in *Arabidopsis*. (A) Schematic diagram of Cre site-specific recombination at *loxP* direct repeats. Recombination results in liberation of a circular molecule containing one of the *loxP* sequences and the DNA from between the two *loxP* sequences. (B) Target site construct AGLox. The two *loxP* sequences are indicated by open arrows, and the 35S::GUS gene and associated restriction sites are indicated. The *AGAMOUS* (*AG*) clone (not drawn to scale) was inserted at the *Pme*I site. (C) Heat shock::CRE gene fusion construct. The HSP 18.2 promoter was fused to the CRE coding region, and attached to a 3′ NOS terminator.

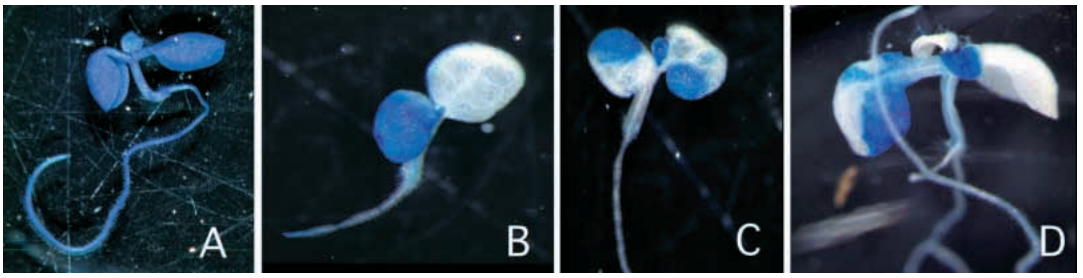

Fig. 2. Seedlings containing GUS(–) sectors induced during embryogenesis. (A) Non heat-shocked control seedling stained for GUS activity shows GUS staining throughout all organs. (B) GUS-stained seedling heat-shocked 4 days after pollination. Note that one cotyledon is almost entirely white (non-stained), suggesting that it arose from an early excision event. (C,D) GUS-stained seedlings heat shocked 5 days after pollination.

characterized clonal relationships between the L1, L2 and L3 meristematic layers and floral organs that have been described for other species (Satina et al., 1940; Satina 1944; Dermen and Stewart, 1973; Tilney-Bassett, 1986) and supported by studies in *Arabidopsis* (Hill and Lord, 1989; Bouhidel and Irish, 1996). Because the L1 gives rise to the epidermis and the L2 to subepidermal cells, and because the 35S promoter provides strong expression in mature sepals (Fig. 4C), presence of the GUS staining product in sepal epidermal and subepidermal cells was used as an indicator of an intact AGLox construct in the L1 and L2, respectively. Frequently, plants with an L2(–) sector also showed GUS staining in vascular-associated cells (Fig. 6D,F). Staining of these cells could indicate that the GUS enzyme or product is transported through the phloem or that these stained vascular tissues are L3-derived. L3-derived cells primarily make up the inner core of the flower and portions of the carpels, therefore presence of the GUS staining product in the receptacle core was used to indicate that the L3 contained the intact AGLox construct. Furthermore, because of the possibility of mericlinal sectors (sectors that are only present in part of a flower), only flowers that showed a consistent sector configuration in all four sepals were included in our analysis.

Mosaic plants produce flowers with at least two different *ag* phenotypes

To generate the plant material for *ag* mosaic analysis, we crossed [AGLox/AGLox; *ag-3*/*ag-3*] plants with [HS::CRE/HS::CRE; *ag-3*/+] plants. F_1 seedlings were heat-shocked 4 days after germination, grown until about 10 flowers were open, and examined for the presence of *ag* mutant flowers. Strong *ag* mutants produce indeterminate flowers (flowers with an increased number of whorls of organs) containing only sepals and petals (compare the wild-type flower in Fig. 5A with the *ag-3* flower in Fig. 5B). Among the controls performed to test the system, we showed (1) that the AGLox construct rescued the *ag* mutant phenotype, except for an occasional modest loss of determinacy (see below), (2) heat-shock of more than 100 [AGLox/AGLox; *ag-3/ag-3*] plants did not result in any *ag* mutant plants, and (3) heat shock of more than 100 [HS::CRE/HS::CRE] plants did not result in the production of any *ag*-like flowers.

In one experiment using F_1 seedlings (as described above), 28 seedlings were not heat-shocked and 83 were heat-shocked. All non-heat shocked flowers showed wild-type organ identity, although some flowers on six of these control plants showed an increased carpel number. Increases in carpel number could reflect a partial loss of floral determinacy. Among 83 heat-shocked plants, 51 had three or more flowers that showed *ag*-like defects in the third and fourth whorls (Fig. 5C-F). The putative mosaics contained a variable number of mutant flowers that generally appeared along one side of the primary inflorescence and frequently extended into one or more secondary inflorescences. In addition, flowers adjacent to the *ag*-like mutant flowers often

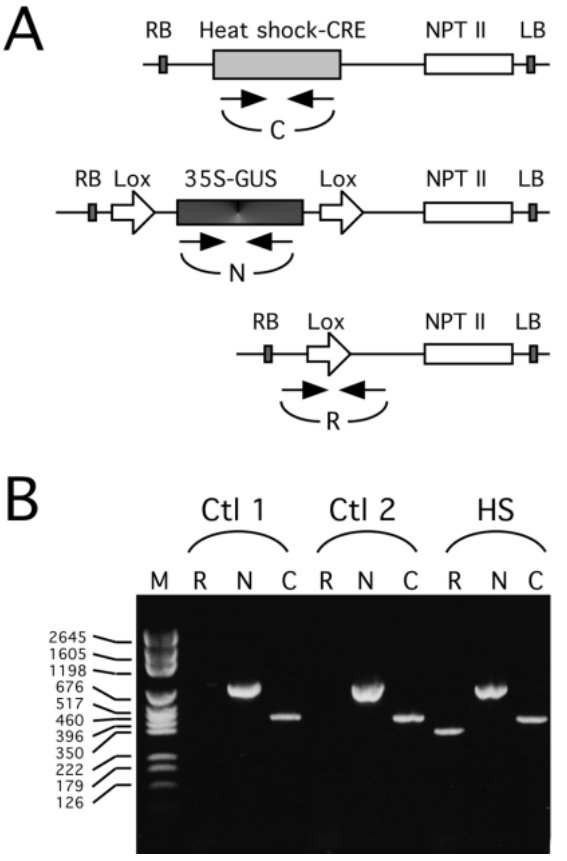

Fig. 3. Transmission of the Cre-induced sector into inflorescence tissue. (A) Schematic representation of oligonucleotide pairs used to assay for constructs in inflorescence tissue; (B) Products of PCR reactions using the oligonucleotide pairs depicted in A and DNA isolated from inflorescence tissue of two non-heat-shocked controls (Ctl 1 and Ctl 2) and one heat-shocked plant (HS). All three samples gave the anticipated 400 bp product for the 'C' reaction, and the 702 bp product for the 'N' reaction, indicating that these tissues contained both the HS::CRE transgene and the non-recombined construct. In contrast, only DNA isolated from the heat-shocked plants produced the 330 bp 'R' product, indicative of recombination.

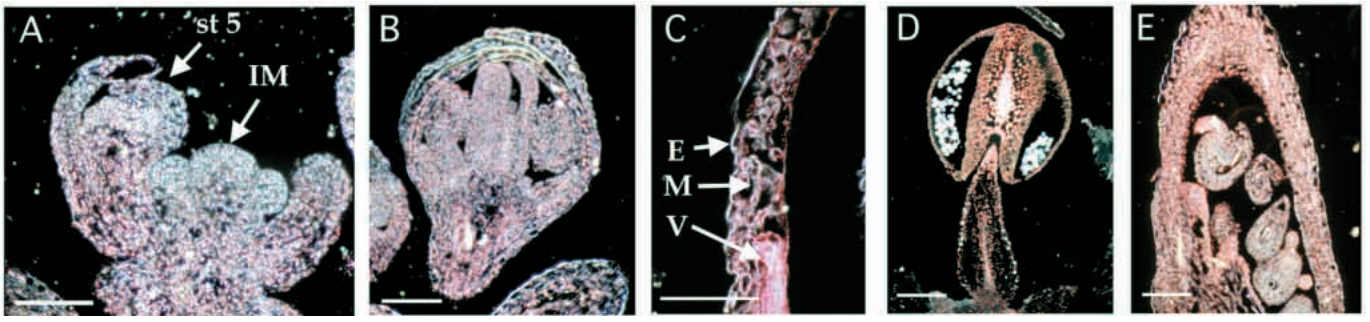

Fig. 4. Dark-field views of GUS staining conferred by 35S::GUS. (A) A section through the inflorescence meristem (IM), two very young floral primordia, and a stage 5 flower (st5). Note the very low levels of GUS staining, seen as orange dots, in both the inflorescence and floral meristems. (B) A stage 7 flower shows more uniform and stronger GUS staining than earlier floral stages. (C) The sepal of a stage 9 flower shows GUS staining in epidermal (E), mesophyll (M), and vascular-associated cells (V). (D) A stamen from a flower at anthesis shows nearly uniform GUS staining. (E) Developing carpel with ovules shows a somewhat variable and moderate intensity of GUS staining. Size bars, 100 μm.

showed a fourth whorl composed of more than 2 carpels (Fig. 5D), suggesting some loss of determinacy.

The mutant flowers fell into three phenotypic classes. The major classes were (1) a strong mutant, which was indistinguishable from the strong *ag-3* allele (Fig. 5C-E; compare to the *ag-3* flower in Fig. 5B), and (2) a novel *ag* mutant, which had outer flowers that resembled the strong *ag* mutant (sepals-petals-petals), and internal flowers that contained variable amounts of carpelloid (Fig. 5E) and/or staminoid tissue (Fig. 5F). Occasionally, both classes appeared within the same inflorescence (Fig. 5E). A third class had indeterminate flowers composed of all 4 organ types; the carpels on these flowers typically burst open to reveal the organs inside. The variability of phenotypes among the putative mosaics suggested that there might be different consequences for the loss of *AG* activity in different layers of the meristem. To determine the sector types that result in these floral phenotypes, we analyzed the cellular distribution of GUS activity, which served as an indicator of wild-type *AG* cells.

Sector configuration of mosaic plants with strong *ag* mutant flowers

The sector configurations of 42 flowers with the strong *ag* phenotype from 15 different mosaic plants were determined for the outer flower (whorls 1-3); data and sector nomenclature are summarized in Table 1. Five different sector types were identified. Thirteen flowers from 6 plants had no detectable GUS staining cells (Fig. 6B), indicating that all cells that contributed to those flowers had undergone excision of their AGLox construct (the L1/2/3(–) mosaic configuration), and thus the flowers were genetically identical to the strong *ag-3* mutant. 29 strong *ag* flowers exhibited GUS staining (and thus some *AG* wild-type cells) in one or more layers. Among these, 20 flowers from 11 plants had the L2(–) sector configuration (Fig. 6C,D); 3 flowers from 2 plants had the L2/3(–) sector configuration (Fig. 6E,F) although occasional inconsistencies with the youngest internal flowers were noted (Fig. 6E); and 6 flowers from 2 plants had the L1/2(–) sector configuration (data not shown). The one feature common to all the sector configurations resulting in strong *ag* mutant flowers is the absence of *AG* in the L2-derived cells. This result suggested that for normal flower development, there is a critical requirement for *AG* in the L2.

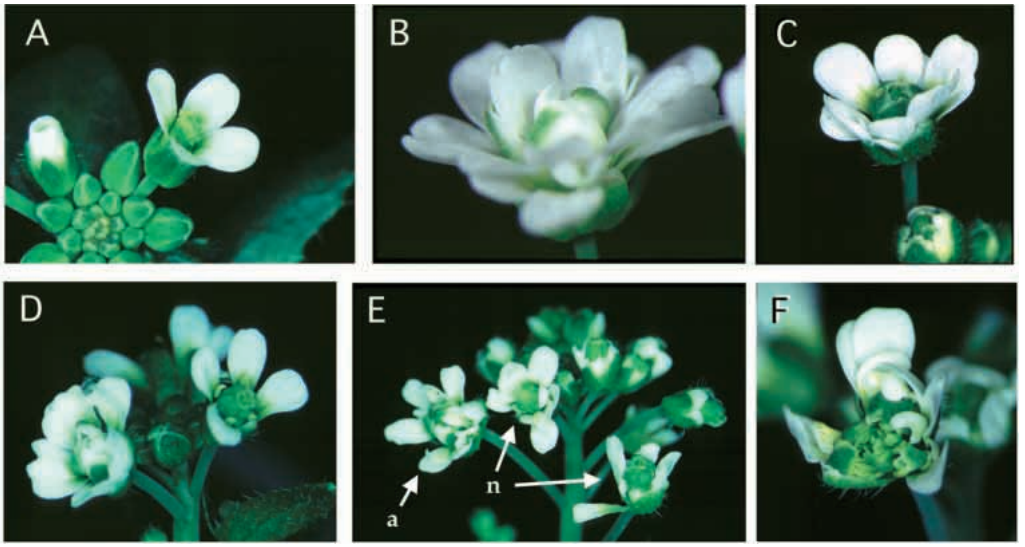

Fig. 5. Phenotypes observed in mosaic flowers. (A) An inflorescence from a wild-type (Landsberg *erecta*) plant. (B) A flower from an *ag-3* plant, composed of many whorls of sepals and petals. (C) An *ag-3*-like flower from a mosaic plant. (D) An inflorescence showing an *ag-3*-like flower (on the left) and a flower with all four organ types (upper right), note that the fourth-whorl carpels are very fat, consistent with a loss of floral meristem determinacy. (E) An inflorescence showing both an *ag-3*-like flower (a), and a novel *ag*-like flower (n) composed of sepals, and petals in their outer flower, and large carpelloid organs in the position of the internal flower. (F) A flower from the novel class of mosaics; the outer 3 whorls contained sepals, petals, petals, and the internal flowers contain sepals and staminoid tissue.

Sector configuration of mosaics with a novel *ag* phenotype

The sector structures of 136 flowers with the novel *ag* phenotype (outer flower showed strong *ag* phenotype, internal flowers had variable amounts of carpelloid and staminoid organs) from 26 different mosaic plants were determined for the outer flower. In all 136 flowers, the outer flowers exhibited just two different types of sector configurations (Table 1). Five of the flowers (from four mosaic plants) had the L2/3(–) sector configuration in the outer flower (data not shown), and 131 flowers from 26 mutant plants had the L2(–) sector configuration in the outer flower (Fig. 6G,H). The features in common between these two sector types are the loss of *AG* in the L2 and the presence of *AG* in the L1.

The difference between the strong and novel *ag* mosaic flowers resulted from the restoration of *AG* expression in the L2 of the inner flowers. That is, the outer flower sector pattern [L2(–) or L2/3(–)] was eventually replaced by a sector pattern with GUS staining (and therefore *AG*) in the L2 (Fig. 6G-J). Similar restoration of *AG* in the L2 was also occasionally observed for the innermost organs of strong *ag* L2(–) mosaics (Fig. 6E); these flowers probably would have produced staminoid and carpelloid organs had their development continued. There are two possible explanations for the sector pattern change. These flowers could have contained a small L2 mericlinal sector with an intact AGLox construct that contributed a major portion of the internal flowers; alternatively, the change in sector configuration could have arisen by L2 layer invasion by cells from another layer during the development of the flower. Based on the frequency with which the sector structure of outer and inner flowers differed, the pre-screening criteria that all four sepals show a consistent sector structure for inclusion in this study, and the frequency with which layer invasion has been observed in other systems (Tilney-Bassett 1986; Hantke et al., 1995; Perbal et al., 1996), we propose that layer invasion is the most important contributor to this change in sector structure.

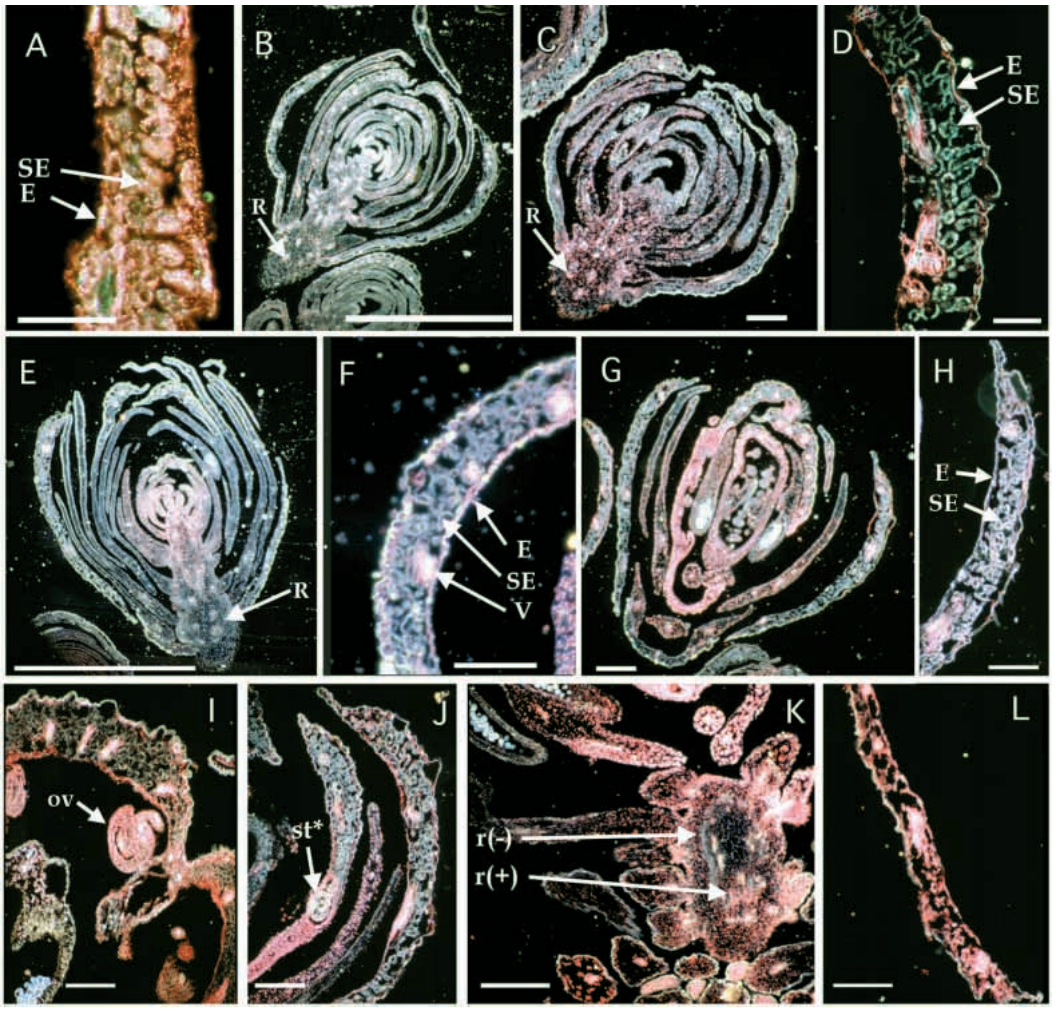

Fig. 6. Mosaic sectors of *ag* mutant flowers. To identify whether each layer contained a wild-type *AG* gene, GUS staining was assessed in the tissues that are derived from each layer. Because the L1 and the L2 give rise to the epidermal (E) and subepidermal (SE) tissues, respectively, we used GUS staining in the sepals to assess whether the L1 and L2 carried a wild-type *AG* gene. The sepal GUS staining pattern from a non-heat-shock control plant is shown in A; uniform GUS staining was observed in the L1-derived epidermal cells (E), and in the L2-derived subepidermal cells (SE). To determine whether the L3-derived cells carried a wild-type *AG* gene, we assessed GUS staining in the core of the receptacle (R in B); for control plants, this GUS staining was uniform (data not shown). (B) Large strong *ag* mutant flower with no layers showing GUS staining. (C) A flower showing a strong *ag* mutant phenotype and an L2(–) sector structure. (D) A section through the sepal of the flower shown in C. (E) A flower showing a strong *ag* mutant phenotype, and an L2/3(–) sector structure. (F) A higher magnification view of a section through the same flower as shown in E. (G) A flower showing the novel *ag* phenotype, and an L2(–) sector structure (R not shown). (H) A higher magnification view of the sepal from the flower shown in G. (I) A section through a mosaic flower showing the novel *ag* phenotype and bearing carpelloid structures (note ovule; ov). (J) A section through a different mosaic flower showing the novel *ag* phenotype; a staminoid sector can be observed in the sepal of an internal flower (staminoid sector is labeled st*). (K) A section showing a plant with a mericlinal sector through the L3; r(-) indicates the part of the receptacle core that is not GUS stained, and r(+) indicates the part of the receptacle core that is GUS stained. (L) A higher magnification view of the sepal from the flower shown in K. Bars, (B, E) 1 mm; (C,G,K) 200 μm; (A,F,H,I,J,L) 100 μm; (D) 50 μm.

Table 1. Periclinal sector configurations

Sector designation	GUS and AG expression* L1	L2	L3	Number of flowers showing a strong ag phenotype†	Number of flowers showing "novel" ag phenotype†	Number of flowers showing indeterminate flowers but all floral organ types†
L1/2/3(–)	(–)	(–)	(–)	13 (6)		
L2/3(–)	(+)	(–)	(–)	3 (2)	5 (4)	
L1/3(–)	(–)	(+)	(–)			
L1/2(–)	(–)	(–)	(+)	6 (2)		
L3(–)	(+)	(+)	(–)			3 (2)
L2(–)	(+)	(–)	(+)	20 (11)	131 (26)	
L1(–)	(–)	(+)	(+)			

*(+) refers to the presence of GUS staining, indicating an intact *AG* gene and (–) refers to the absence of GUS staining and the loss of an intact *AG* gene.
†Numbers in parentheses refer to the number of different mosaic plants showing this class of mutant flower with the assigned sector configuration; some plants contained flowers with more than one type of periclinal chimera.

Sector configuration of the indeterminate mosaic flowers

Three flowers from two mosaic plants contained stamens and carpelloid tissue in the outer flower, yet were indeterminate; these flowers showed an L3(–) sector configuration (Table 1; Fig. 6K,L). We observed abnormal carpelloid structures in these flowers; this observation suggests that at least some features of carpels can be specified by the presence of a functional *AG* gene in the L1 and L2, but that a normal fused carpel requires *AG* expression in all three layers. In addition, the loss of determinacy in these flowers suggested that *AG* in the L3 is necessary for flower determinacy. However, *AG* in this position is not sufficient for determinacy, as L2(–) and L1/2(–) flowers are also indeterminate.

Non-autonomy of mutant L2 sectors

The most commonly observed mosaic, L2(–), contained 10 petals in its outer flower (as compared to 4 petals and 6 stamens in wild type). Because the epidermal morphology of petals and stamens are distinct (Smyth et al., 1990), we were able to ask whether the epidermal cells of L2(–) mosaic third whorl organs differentiated into stamen-like epidermal cells, suggesting differentiation according to their own wild-type *AG* genotype, or whether they differentiated as petal-like epidermal cells, suggesting that they responded to signals from the L2. Fig. 7A and B show DIC images of petal and stamen epidermal cells of a wild-type plant; petal epidermal cells appear domed whereas the stamen epidermal cells are flat. In the L2(–) mosaic, all 10 petal organs had domed epidermal cells that were indistinguishable from those of wild-type petals (Fig. 7C). In the staminoid petals that occasionally arose in internal flowers of the novel *AG* mosaic phenotypic class, appearance of GUS-staining cells along the margin of the organ coincided with a small sector of staminoid tissue and the typical staminoid epidermal cells (Fig. 7D). These results indicate that the identity of third whorl epidermal cells was communicated by the *ag* genotype in the L2, and not the *AG* genotype of the L1.

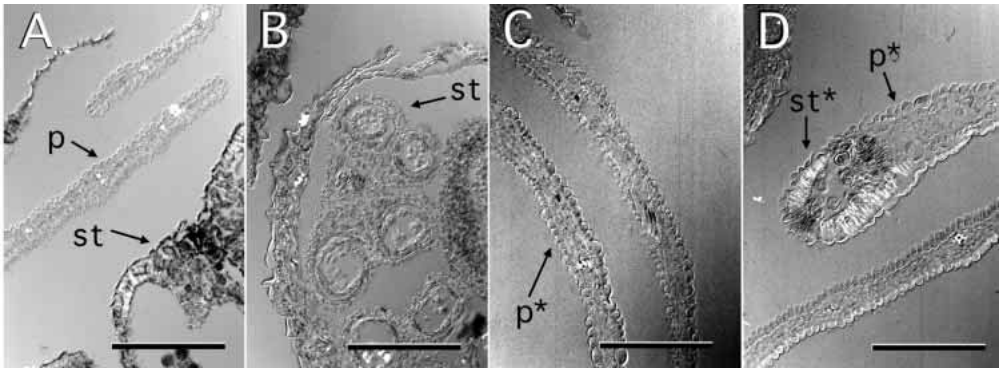

Fig. 7. Epidermal cell identity in third whorl organs of mosaic flowers. (A) Epidermal cells of petals and stamens can be distinguished by the domed surface of the petal cells (p) in contrast to the flat epidermal cells of stamens (st). (B) Stamen epidermal cell morphology from a younger wild-type flower. (C) A section through the outer flower of a novel *ag* mosaic flower. Two organs with typical petal epidermal cells are shown; the same epidermal cell morphology was observed for all 10 petal-like organs. p* indicates an organ that presumably arose in the third whorl. (D) A chimeric organ from an internal L2(–) flower; most of the epidermal cells look identical to normal petal epidermal cells (p*), except at the distal end where a small GUS-staining sector gave rise to staminoid tissue (st*). Bars (A-D) 100 μm.

DISCUSSION

AG functions non-autonomously during development

The goal of this study was to determine which meristematic cell layers (L1, L2, L3) require *AG* function for normal flower development. We used a Cre/*loxP* strategy to study *ag* mosaic plants, and determined that *AG* is required in the L2 for stamen and carpel development, and is required in both the L2 and the L3 for floral meristem determinacy. Among the 178 mutant mosaic flowers from 27 mosaic plants, no epidermal (L1-derived) sector was identified (Table 1). There are at least three possible explanations for this: (1) epidermal (L1-derived) cells differentiate based on non-autonomous action of *AG* in

another layer; (2) *AG* is required in the L1 for normal development, but we have not examined enough mosaic plants to find the L1(–) mutants; or (3) artifacts from GUS staining prevent detection of this pattern. We occasionally observed L1(–) sectors in wild type flowers of multi-sectored inflorescences (data not shown), so if loss of *AG* in the L1 led to a mutant phenotype, this sector would have been identifiable. Furthermore, the repeated recovery of other sector types among the mutants argues that if an L1(–) mosaic led to a mutant phenotype, it should have been among the flowers we analyzed. Taken together, these results suggest that *AG* functions nonautonomously to provide developmental information to the L1.

What is the source of L1 developmental signals?

If the L1 is receiving *AG* developmental information from elsewhere in the developing flower, then the next question is, what is the source of this information? Possible sources include the L2, the L3, or both these layers. An L3 signal is not necessary, as L3(–) sectors did produce staminoid and carpelloid structures; nor is it sufficient, as L2(–) sectors produced no staminoid or carpelloid structures (Table 1). In contrast, the L2 is necessary, as the L2(–) plants did not produce staminoid or carpelloid structures. Corroboration comes from the novel class of *AG* mosaics, where the restoration of *AG* in the L2 was accompanied by the appearance of staminoid and carpelloid tissues. Because some of these internal flowers contained apparently normal stamens, *AG* expression in the L1 and L2 is sufficient for stamen specification. Carpel specification, however, apparently requires more information, as normal-looking carpels in mosaic flowers were rare.

L2 layer invasion

The major feature of the novel class of *ag* mosaic flowers was the appearance of L2(+) cells in the internal flowers while the outer flower was L2(–). We attribute this change in sector structure to layer invasion (see Results). Although invading cells could have derived from either adjacent layer (the L1 or the L3), only L2(–) and L2/3(–) sectors gave rise to the novel phenotype (Table 1), suggesting that the GUS-staining cells originated from the L1. One question that follows from these observations is whether non-standard periclinal divisions in the L1 were influenced by *ag* mutant sectors. That our observations of layer invasion were restricted to the inner proliferating flowers suggests that the indeterminate growth caused by the loss of *ag* function correlates with a breakdown of normal patterns of cell division. Other studies have also observed that specific genotypes can influence cell division patterns. Periclinal mosaics using two different genotypes of tobacco showed that specific genotype orientations led to L2 invasion from the L3 (Marcotrigiano and Bernatzky, 1995). In maize, mosaic analysis of the dominant mutant *Kn1* showed that ectopic leaf expression of *Kn1* in internal cells results in an abnormal proliferation of (L1) epidermal cells (Sinha and Hake 1990).

Floral determinacy

One feature of all *ag* mutants, and L2(–), L3(–) and L2/3(–) mosaics, is a defect in cessation of floral meristem proliferation after the production of four whorls of organs. This loss of floral meristem determinacy in mosaic flowers indicates that producing a determinate floral meristem depends on receiving the appropriate signals from both the L2 and the L3. Other studies examining *AG* functions have suggested that for normal determinacy, high levels of *AG* are required (Sieburth et al., 1995; Mizukami and Ma, 1995). Furthermore, this high level of *AG* must be within the fourth whorl itself, as expression of *AG* in the third whorl, but not the fourth, is not sufficient to confer floral meristem determinacy (Jack et al., 1997). Our studies extended these observations by showing that the determinacy conferring activity must be present in both the L2 and the L3.

The quantitative requirement for *AG* in specification of determinacy, combined with its biochemical function as a DNA binding protein (Mueller and Nordheim 1991; Huang et al., 1993; Shiraishi et al., 1993), suggests that *AG* might confer determinacy through the negative regulation of a gene whose product promotes meristem identity or cellular proliferation. Furthermore, that either L2(–) or L3(–) sectors result in loss of determinacy also suggests that this putative meristem proliferation gene acts non-autonomously. A candidate for the putative proliferation gene is that it is a member of the KN/STM family of homeodomain proteins. Members of this gene family have roles in meristem specification or maintenance (Smith et al., 1992; Sinha et al., 1993; Barton and Poethig, 1993; Long et al., 1996; Überlacker et al., 1996; Müller et al., 1995; Clark et al., 1996). Strong candidates include the *Arabidopsis* homologs of *ZmHox1* (from maize) or the *Knox3* gene of barley; for both of these genes, ectopic expression phenotypes include additional flowers within their flowering structures (Überlacker et al., 1996; Müller et al., 1995). An intriguing correlation between ectopic expression of the homeodomain gene *Kn1* and the *ag* mosaic flowers is the proliferation of L1-derived cells. Mosaic analysis showed that ectopic leaf expression of *Kn1* in the L3 results in an abnormal proliferation of L1 cells (Sinha and Hake, 1990). If the loss of *AG* in the L2 or the L3 resulted in ectopic expression of a gene such as *Kn1*, then this might provide an explanation of the inappropriate patterns of L1 cell division that we observed.

Is cross-layer signaling a general phenomenon in normal flower development?

Although only a modest number of different plant genes have been studied to assess cell autonomy of specific gene action, some of these analyses have included flower developmental control genes. Transposon excision was used to analyze mosaics of the Antirrhinum gene *FLORICAULA* (*FLO*), which is required for floral meristem identity. Three different revertant flower phenotypes were recovered (Carpenter and Coen, 1995; Hantke et al., 1995). The analysis of these mosaic plants demonstrated that some aspects of *FLO* function were non-autonomous [restoration of a wild-type *FLO* allele in any of the three layers (L1, L2, or L3) resulted in pigmented epidermal petal cells (Carpenter and Coen, 1995), and restoration of *DEF* and *PLE* expression (downstream genes) in all three layers (Hantke et al., 1995)] while other aspects of *FLO* function were cell autonomous (*FLO* autoregulation).

Mosaic analyses have also been performed to assess the autonomy of action of the class B components of the ABC

model for flower development. There are two class B genes, and they function along with the class A genes in the second whorl (to specify petal identity) and function along with the class C gene (*AG*) in the third whorl (to specify stamen identity, reviewed in Coen and Meyerowitz, 1991). In *Arabidopsis*, X-ray treated plants that were heterozygous for one of the class B genes, *PISTILLATA*, failed to result in plants bearing mutant flowers, and led to the suggestion that *PISTILLATA* might function non-autonomously in the L1 (Bouhidel and Irish, 1996). In Antirrhinum, unstable transposon-tagged alleles of the two class B genes, *DEFICIENS* (*DEF*) and *GLOBOSA* (*GLO*) were used to assess cell autonomy of gene action (Perbal et al., 1996). The restoration of normal *DEF* or *GLO* activity in the L2 and L3 layers was sufficient to confer normal development to mutant L1 (epidermal) cells; this result is very similar to the conclusions that we reached regarding *AG* function. In contrast with our results, however, mosaics with mutant cells in the L2 and L3, and the wild-type gene restored in the L1, also showed normal epidermal cell development. The difference between the action of *DEF* and *GLO* in the L1 as compared to *AG* might be reconciled by consideration of the ABC flower development model. One of the proposed functions of *AG*, a class C gene, is to negatively regulate the activity of the class A genes. That *AG* in the L1 of L2(–) mosaics failed to influence epidermal cellular differentiation might result from the loss of negative regulation of the class A genes in the L2, and this ectopic Class A activity functions non-autonomously to supply developmental information to the L1. With the advent of the versatile Cre/*loxP* system for genetic mosaic analysis, this possibility can now be addressed experimentally.

We gratefully acknowledge members of the Meyerowitz lab for useful discussions of this work, and Dr Robert Goldberg, in whose lab the plant transformations were performed. This work was supported by a grant from the National Institutes of Health (GM45697 to E. M. M.), a grant from the National Sciences and Engineering Research Council of Canada (OGP0170655 to L. E. S), by a Damon Runyon-Walter Winchell Cancer Research Fellowship (DRG1081 to L. E. S.), and by an NIH Postdoctoral Fellowship (GM13100-03 to G. N. D.). We also thank Jennifer Fletcher, Doris Wagner, Jose-Luis Reichmann, Toshiro Ito, Kevin Roberg, and Prakash Kumar for critical reading of the manuscript.

REFERENCES

Barton, M. K. and Poethig, R. S. (1993). Formation of the shoot apical meristem in *Arabidopsis thaliana*: an analysis of development in the wild type and in the *shoot meristemless* mutant. *Development* **119**, 823-831.

Benfey, P. N., Ren, L. and Chua, N.-H. (1989). The CaMV 35S enhancer contains at least two domains which can confer different developmental and tissue-specific expression patterns. *EMBO J.* **8**, 2195-2202.

Benfey, P. N., Ren, L. and Chua, N.-H. (1990). Tissue-specific expression from CaMV 35S enhancer subdomains in early stages of plant development. *EMBO J.* **9**, 1677-1684.

Bossinger, G. and Smyth, D. R. (1996). Initiation patterns of flower and floral organ development in *Arabidopsis thaliana*. *Development* **122**, 1093-1102.

Bouhidel, K. and Irish, V. F. (1996). Cellular interactions mediated by the homeotic *PISTILLATA* gene determine cell fate in the *Arabidopsis* flower. *Dev. Biol.* **174**, 22-31.

Carpenter, R. and Coen, E. S. (1995). Transposon induced chimeras show that *floricaula*, a meristem identity gene, acts non-autonomously between cell layers. *Development* **121**, 19-26.

Clark, S. E., Jacobsen, S. E., Levin, J. Z. and Meyerowitz, E. M. (1996). The *CALAVATA* and *SHOOT MERISTEMLESS* loci competitively regulate meristem activity in *Arabidopsis*. *Development* **122**, 1567-1575.

Coen, E. S. and Meyerowitz, E. M. (1991). The war of the whorls: genetic interactions controlling flower development. *Nature* **353**, 31-37.

Dellaporta, S. L., Wood, J. and Hicks, J. B. (1983). Isolation of DNA from higher plants. *Plant Molec. Biol. Reporter* **4**, 19-21.

Derman, H. and Stewart, R. N. (1973). Ontogenetic study of floral organs of peach (*Prunus persica*) utilizing cytochimeral plants. *Amer. J. Bot.* **60**, 283-291.

Drews, G. N., Bowman, J. L. and Meyerowitz, E. M. (1991). Negative Regulation of the Arabidopsis homeotic gene *AGAMOUS* by the *APETALA2* product. *Cell* **65**, 991-1002.

Furner, I. J. and Pumfrey, J. E. (1993). Cell fate in the inflorescence meristem and floral buttress of *Arabidopsis thaliana*. *Plant J.* **4**,917-931.

Golic, K. G. and Lindquist, S. (1989). The FLP recombinase of yeast catalyzes site-specific recombination in the Drosophila genome. *Cell* **59**, 499-509.

Hantke, S. S., Carpenter, R. and Coen, E. S. (1995). Expression of *floricaula* in single cell layers of periclinal chimeras activates downstream homeotic genes in all layers of floral meristems. *Development* **121**, 27-35.

Hill, J. P. and Lord, E. M. (1989). Floral development in *Arabidopsis thaliana*: A comparison of the wild type and the homeotic pistillata mutant. *Can J. Bot.* **67**, 2922-2936.

Huang, H., Mizukami, Y. and Ma, H. (1993). Isolation and characterization of the binding sequences for the product of the Arabidopsis floral homeotic gene *AGAMOUS*. *Nucleic Acids Res.* **21**, 4769-4776.

Irish, V. F. and Sussex, I. M. (1992). A fate map of the *Arabidopsis* embryonic shoot apical meristem. *Development* **115**, 745-753.

Jack, T., Sieburth, L. and Meyerowitz, E. (1997). Targeted misexpression of *AGAMOUS* in whorl 2 of *Arabidopsis* flowers. *Plant J.* **11**, 825-839.

Jefferson, R. A., Kavanagh, T. A. and Bevan, M. W. (1987). GUS fusions: β-glucuronidase as a sensitive and versatile gene fusion marker in higher plants. *EMBO J.* **6**, 3901-3907.

Long, J. A., Moan, E. I., Medford, J. I. and Barton, M. K. (1996). A member of the KNOTTED class of homeodomain proteins encoded by the *STM* gene of *Arabidopsis*. *Nature* **379**, 66-69.

Marcotrigiano, M. and Bernatzky, R. (1995). Arrangement of cell layers in the shoot apical meristems of periclinal chimeras influences cell fate. *Plant J.* **7**, 193-202.

McBride, K. E. and Summerfelt, K. R. (1990). Improved binary vectors for *Agrobacterium*-mediated plant transformation. *Plant Mol. Biol.* **14**, 269-276.

Mizukami, Y. and Ma, H. (1995). Separation of *AG* function in floral meristem determinacy from that in reproductive organ identity by expressing antisense *AG* RNA. *Plant Mol. Biol.* **28**, 767-784.

Mueller, C.G.F. and Nordheim, A. (1991). A protein domain conserved between yeast MCM1 and human SRF directs ternary complex formation. *EMBO J.* **10**, 4219-4229.

Müller, K. J., Romano, N., Gerstner, O., Garcia-Maroto, F., Pozzi, C., Salamini, F. and Rohde, W. (1995). The barley *Hooded* mutation caused by a duplication in a homeobox gene intron. *Nature* **374**, 727-730.

Odell, J., Caimi, P., Sauer, B. and Russell, S. (1990). Site-directed recombination in the genome of transgenic tobacco. *Mol. Gen. Genet.* **223**, 369-378.

Perbal, M.-C., Haughn, G., Saedler, H. and Schwarz-Sommer, Z. (1996). Non-cell-autonomous function of the *Antirrhinum* floral homeotic proteins *DEFICIENS* and *GLOBOSA* is exerted by their polar cell-to-cell trafficking. *Development* **122**, 3433-3441.

Russell, S. H., Hoopes, J. L. and Odell, J. T. (1992). Directed excision of a transgene from the plant genome. *Mol. Gen. Genet.* **234**, 49-59.

Satina, S., Blakeslee, A. F. and Avery, A. G. (1940). Demonstration of the three germ layers in the shoot apex of datura by means of induced polyploidy in periclinal chimeras. *Amer. J. Bot.* **27,** 895-905.

Satina, S. (1944). Periclinal Chimeras in Datura in relation to Development and Structure (A) of the Style and Stigma (B) of Calyx and Corolla. *Amer. J. Bot.* **31**, 493-502.

Shiraishi, H., Okada, K. and Shimura, Y. (1993). Nucleotide sequences recognized by the AGAMOUS MADS domain of Arabidopsis thaliana in vitro. *Plant J.* **4**, 385-398.

Sieburth, L. E., Running, M. P. and Meyerowitz, E. M. (1995). Genetic separation of third and fourth whorl functions of *AGAMOUS*. *Plant Cell* **7**, 1249 – 1258.

Sieburth, L. E. and Meyerowitz, E. M. (1997). Molecular dissection of the *AGAMOUS* control region shows that *cis* elements for spatial regulation are located intragenically. *Plant Cell* **9**, 355-365.

Sinha, N. and Hake, S. (1990). Mutant characters of *Knotted* maize leaves are determined in the innermost tissue layers. *Dev. Biol.* **141**, 203-210.

Sinha, N., Williams, R. E. and Hake, S. (1993). Overexpression of the maize homeobox gene, *KNOTTED-1*, causes a switch from determinate to indeterminate cell fates. *Genes Dev.* **7**, 787-795.

Smith, L. G., Greene, B., Veit, B. and Hake, S. (1992). A dominant mutation in the maize homeobox gene, *Knotted-1*, causes its ectopic expression in leaf cells with altered fates. *Development* **116**, 21-30.

Smyth, D. R., Bowman, J. L. and Meyerowitz, E. M. (1990). Early flower development in *Arabidopsis*. *Plant Cell* **2**, 755-767.

Sternberg, N. and Hamilton, D. (1981). Bacteriophage P1 site-specific recombination I. Recombination between *loxP* sites. *J. Mol. Biol.* **150**, 467-486.

Takahashi, T. and Komeda, Y. (1989). Characterization of two genes encoding small heat-shock proteins in *Arabidopsis thaliana*. *Mol. Gen. Genet.* **219**, 365-372.

Tilney-Bassett, R. A. E. (1986). *Plant Chimeras*. London: Edward Arnold.

Überlacker, B., Klinge, B. and Werr, W. (1996). Ectopic expression of the maize homeobox genes *ZmHox1a* and *ZmHox1b* causes pleiotropic alterations in the vegetative and floral development of transgenic tobacco. *Plant Cell* **8**, 349-362.

Valvekens, D., Van Montague, M. and Van Lijsebettens, M. (1988). Agrobacterium tumefaciens-mediated transformation of *Arabidopsis thaliana* root explants by using kanamycin selection. *Proc. Natl. Acad. Sci. USA* **85**, 5536-5540.